15 March 2002

ELSEVIER

Optics Communications 203 (2002) 377–384

OPTICS COMMUNICATIONS

www.elsevier.com/locate/optcom

Effect of ruthenium doping on the optical and photorefractive properties of $Bi_{12}TiO_{20}$ single crystals

V. Marinova [a,*,1], Mei-Li Hsieh [a], Shiuan Huei Lin [b], Ken Yuh Hsu [a]

[a] *Institute of Electro-Optical Engineering, National Chiao Tung University, 1001 Ta Hsueh Road, Hsinchu 30050, Taiwan*
[b] *Department of Electrophysics, National Chiao Tung University, 1001 Ta Hsueh Road, Hsinchu 30050, Taiwan*

Received 16 January 2002; received in revised form 16 January 2002; accepted 23 January 2002

Abstract

$Bi_{12}TiO_{20}$ (BTO) single crystals nominally pure and doped with ruthenium are grown by top-seeded solution growth method. The effect of ruthenium concentration on optical and photorefractive properties is studied. Strong influence of doping on these properties is observed. It is shown that optical transmission of crystal samples with higher ruthenium content is shifted to the near IR spectral region, while the absorption coefficient is considerably increased. The optical activity of Ru doped crystals is further reduced in comparison with undoped BTO. Photochromic effect is observed in strongly doped crystal. Photorefractive properties are experimentally investigated using two-beam coupling. Response time and diffraction efficiency are changed with ruthenium content.

Keywords: Single crystals; Doping elements; Optical properties; Photochromic effect; Photorefractive properties

1. Introduction

Bismuth oxide compounds with chemical composition $Bi_{12}MO_{20}$ (where M = Si, Ge, Ti) crystallize on *I23* space group, known as sillenite structure. Among other photorefractive crystals, such as $LiNbO_3$ and $BaTiO_3$, sillenites attract special interest owing to a higher photosensitivity and high carrier mobility, which permit achievement of fast response time and wide applications in real-time holography, coherent light amplification, optical phase conjugation, optical information processing, optical interconnection and communications, etc., [1–3]. Moreover sillenites can be easily doped and thus the crystal properties can be tailored in a desired direction.

In comparison with other sillenites, $Bi_{12}TiO_{20}$ (BTO) crystals are most promising because of higher photoconductivity, electro-optical coefficients and holographic sensitivity in the red spectral region, which suits the wavelengths of the low-cost and commonly used He–Ne and diode lasers [4]. Furthermore, the optical activity in BTO is considerably lower than in $Bi_{12}SiO_{20}$ (BSO) and

* Corresponding author. Tel.: +886-3-5712121x56329; fax: +886-3-5716631.

E-mail addresses: vera@cc.nctu.edu.tw, vera_marinova@yahoo.com (V. Marinova).

[1] On leave from Central Laboratory of Optical Storage and Processing of Information, Bulgarian Academy of Sciences, 1113 Sofia, Bulgaria.

0030-4018/02/$ - see front matter
PII: S0030-4018(02)01127-6

$Bi_{12}GeO_{20}$ (BGO) [4,5], making them appropriate media for optical spatial soliton propagation, wave-guides and fiber-like crystals [6].

BTO crystals are photorefractive materials with large energy gap, in which the intrinsic (stoichiometric) defects of the crystal structure act as attractive matrix for many dopants (extrinsic defects), such as transition metal and rare earth elements. Dopants are intentionally incorporated in the crystal structure in order to optimize physical properties. The important dopant factors are their concentration, valence state and the ability to take different valences, distribution coefficient, occupied sites symmetry, etc. The properties of BTO crystals with different doping elements such as Al, Ag, Ga, Fe, Mn, Co, Cr, Cu, Ca, Cd, V, P [7–15] are already investigated and discussed, however up to now a study of Ru influence on BTO properties is still missing. Ruthenium seems to be an interesting dopant since it is reported to improve the photorefractive sensitivity of $KNbO_3$ for red light [16].

The presence of point defects or doping ions in the crystal structure leads to generation of a charge transfer process responsible for photochromic and photorefractive effect – phenomena, which are extensively used in holographic data storage. Inhomogeneous laser illumination created by the interference of the reference and signal beam excites charge carriers from impurity levels into the conduction or valence bands, the charge carriers migrate (by diffusion or drift) and finally are trapped by empty impurities. The resulting space charge field modulates the refractive index via the electro-optic effect. Since the structures and densities of intrinsic defects substantially influence a variety of physical properties, including the photorefractive effect, the relationship between defects and properties is a very important research field, in searching for new and better photorefractive materials.

In this paper we report for the first time, to our knowledge, preliminary experimental results for the effect of two different ruthenium concentrations on optical absorption, optical activity and holographic properties of BTO single crystals. The results are compared with those of undoped BTO.

2. Experimental details

Nominally pure and doped with two different concentrations of ruthenium $Bi_{12}TiO_{20}$ single crystals were grown in a standard Chzochralski apparatus using top-seeded solution growth method (TSSG) [17]. The purity of the starting products Bi_2O_3 and TiO_2 were 99.999% and their proportion was 11:1 in weight. Ruthenium was introduced into the melt solution in the form of RuO_2 and its concentration in the grown crystals determined by atomic absorption spectroscopy is given in Table 1. BTO:Ru(1) and BTO:Ru(2) denote crystals with low and high ruthenium content, respectively, according to Table 1. It was established experimentally that 1×10^{19} cm^{-3} of ruthenium is the maximal allowable concentration for growing the optical homogeneous BTO:Ru crystals.

Transmission spectra were measured on double polished plates with a thickness approximately 1 mm in the wavelength range 0.4–2 μm using Cary 5I spectrophotometer. Reflection spectra were measured on plates with one polished and one grinded side in a visible spectrum using Perkin–Elmer 330 spectrophotometer with special references for calibrations at 488, 514.5, 576, 633 and 672 nm. The absorption coefficient α (cm^{-1}) was calculated using the classical formula

$$T = \frac{(1-R^2)\exp(-\alpha d)}{1+R^2\exp(-2\alpha d)}, \tag{1}$$

where T stands for the transmission coefficient, R for the reflection coefficient and d for the plate thickness.

The optical activity was measured on crystal plates by using laser light sources emitting at 488, 496, 514, 532, 633 and 650 nm, a polarizer, an

Table 1
Description of the crystals used in the experiments

Notation	Ru concentration (cm^{-3})	Dimensions $a \times b \times c$[a] $(mm)^3$
BTO		$8 \times 8 \times 4$
BTO:Ru(1)	1×10^{18}	$8 \times 8 \times 4$
BTO:Ru(2)	1×10^{19}	$7 \times 7 \times 6$

[a] Thickness.

analyzer and photodetector. The angle of rotation of the polarization plane was determined by rotating the analyzer until extinction. The optical rotatory power ρ (deg/mm) was calculated by the ratio of the rotation angle and samples thickness.

Holographic experiments were carried out using a standard two-beam interference set-up. Volume phase holograms were recorded by He–Ne laser source on crystal samples, which edges are oriented with respect to the crystallographic [1 1 0], [0 0 1] and [1 1 0] directions. The crystal's dimensions for holographic storage are given in Table 1. The holographic recording was performed with linear polarization of subject I_S and reference I_R interfering beams with equal intensities in a conventional geometry to obtain maximum diffraction efficiency of sillenites, i.e. the hologram wave vector K_g was perpendicular to the [0 0 1] axis. I_S and I_R beams were incident onto the crystal with the incident angle 2θ varying between 24° and 70°. The elementary holograms were recorded without external electric field, therefore only diffusion mechanism takes part in charge redistribution inside the crystal. During writing the diffraction efficiency of the holograms was monitored by switching off the signal beam (for about 0.05 s) and detecting transmitted (I_{transm}) and diffracted (I_d) intensities of the reference beam. The diffraction efficiency η can be calculated from the detected intensities using the following formula:

$$\eta = \frac{I_d}{I_d + I_{transm}}. \quad (2)$$

All holographic measurements were performed at room temperature.

3. Results and discussion

3.1. Remarks on the crystal structure of BTO

The sillenites have a complex crystal structure that allows the existence of a number of charge trapping sites. The BTO elementary crystal cell is built of two structural units [18–20]:

- TiO_4 tetrahedra: Ti-atoms are located in the corners and at the center of the elementary cell where they occupy the center of tetrahedra, surrounded by four equidistant oxygen O(3) atoms, and
- BiO_5 polyhedron: each of the 24 bismuth atoms is located in the surrounding of five oxygen atoms.

According to the neutron diffraction investigations [21], there are 10% vacancies in undoped BTO in tetrahedral positions that are related to the greater ionic radius of Ti^{4+} ($r_{Ti} = 0.68$ Å) compared with the ionic radius of Ge^{4+} ($r_{Ge} = 0.53$ Å), which is ideal for introduction in a MO_4 tetrahedron of the sillenite structure. Our recent neutron diffraction study [22] established even more vacancies in the case of doped BTO. The presence of such vacancies contributes to the change from an "ideal" bismuth octahedron $BiO_{n=7}$ (such as in BSO and BGO) into a "defective" $BiO_{n=5}$ polyhedron as in the case of BTO. To preserve the electro-neutrality, the Ti^{4+} vacancies in TiO_4 are occupied by Bi^{3+}-atoms, resulting in the emergence of two oxygen O(3) vacancies in the tetrahedron, which are at the same time in polyhedral positions.

Thus, BTO appeared as more defective (the concentration of photoactive centers is higher) than other sillenites, which causes a difference in physical properties.

3.2. Optical properties

3.2.1. Transmission spectra

The transmission dependence on the light wavelength between 0.4 and 2 μm for the undoped and doped with two different concentrations of ruthenium BTO samples is shown in Fig. 1. Calculated values of absorption coefficient at several wavelengths are listed in Table 2. Typical well-defined transmission shoulder is observed in undoped BTO, due to the contribution of intrinsic defects $Bi^{3+} + h^+$ located on a Ti^{4+}-site (h^+ denotes a positive hole on a neighbor oxygen on the M-centered tetrahedron) [14,23]. The transmission edge is shifted to the near IR region with the increasing of Ru content. Similar effect was observed by doping BTO crystals with different concentration of Cu [11]. The IR shift, respectively, the absorption coefficient increasing, probably is due to the photochromism, which is most pronounced in

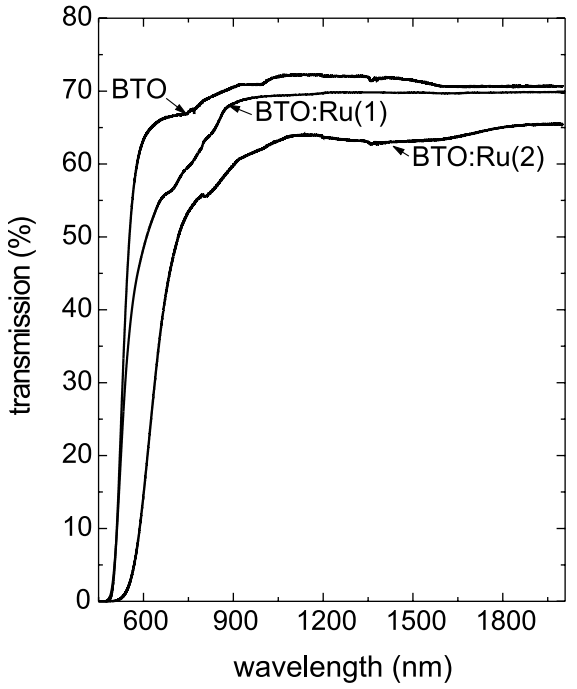

Fig. 1. Transmission spectra of Ru doped BTO in comparison with undoped crystal in spectral range 0.4–2 μm.

Table 2
Calculated values of absorption coefficient α (cm^{-1}) at different wavelengths

Sample α (cm^{-1})	BTO	BTO:Ru(1)	BTO:Ru(2)
542 nm	6.5	8.7	40
633 nm	0.9	2.6	8.7
672 nm	0.5	1.8	4.8

the strongly doped crystals. The photochromic effect appeared as strong dark red coloration of the BTO:Ru(2) crystal. We suppose that the ruthenium ions increase the concentration of effective trap centers and as a consequence the absorption throughout the investigated spectral range increases as the donor concentration increase. Hence, the strongly doped BTO:Ru(2) crystal could be an interesting medium for future investigations in near IR region.

3.2.2. Photochromic effect

The photochromism in an inorganic material is caused by photoinduced charge transfer of electrons (holes) from one localized impurity or defect state in the crystal to another via the conduction (valence) band. The absorption can be changed by illumination because of the redistribution of charge carriers between different traps. The photochromic effect is also reversible from one state to another.

The photochromism in sillenites is associated mainly with the presence of dopants. The undoped crystals also exhibit photochromic effect, however below room temperature [24,25]. In a visible part of the spectrum the phenomenon is due to the photoionization of antisite Bi_M^{3+} defects [26].

In order to confirm the existence of photochromic effect we have measured the transmission and calculated the absorption coefficient α_{ph} (cm^{-1}) difference of oven annealed (at 600 °C, for 30 min) and illuminated with Xenon lamp (150 W) source for 30 min highly doped BTO:Ru(2) crystal samples. It is clearly seen from Fig. 2 that after illumination the absorption coefficient increases (especially in the range between 1.7 and 2.2 eV). The absorption coefficient change after annealing and illumination we suppose is an evidence of the existence of a photochromic effect. Furthermore the magnitude of photochromic absorption increases with the increase of ruthenium concentration. However, the observed effect is weaker than the strong photochromic effect observed in BTO doped with Cr and Mn [26,27].

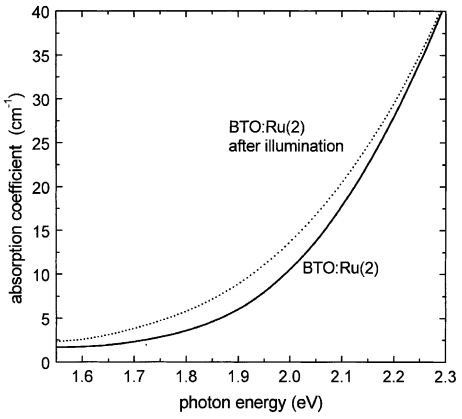

Fig. 2. Change of absorption coefficient α_{ph} of BTO:Ru(2) due to the photochromic effect. Straight line is after annealing at 600 °C, dotted line is after illumination with xenon lamp for 30 min.

3.2.3. Optical activity

Sillenites possess the extremely high value of natural optical activity for inorganic media, leading to a rotation of the polarization planes of the interactive waves.

The optical rotatory power dependence on wavelength for the undoped and ruthenium doped BTO crystals is shown in Fig. 3. The values of optical activity decrease with ruthenium doping. The same behavior is also observed in Ru-doped BSO crystals [12], as well as in BTO doped with Cu, Ag and Co [11].

According to the Burkov theory [28,29], the two structural elements in sillenite structure are considered as basic chromophores, which form chiral complex in the crystal lattice. It is assumed that TiO_4 and "nonsymmetric" BiO_5 chromophores strongly rotate the polarization plane in opposite directions, and "nonsymmetric" BiO_5 polyhedrons have a dominant role in the resulting optical activity. This theory explains also the lower optical activity in BTO in comparison to BSO and BGO.

Generally, TiO_4 tetrahedra appears as achiral clusters in the chiral matrix formed by BiO_5 polyhedron [28,29]. It is supposed that the variation in the optical activity values, due to the vacancies and dopants, is attributed to the changes occurring in the symmetry of these two chromophores. According to the obtained experimental results, probably Ru dopants occupied TiO_4 tetrahedral positions, in the form of achiral clusters embedded in the chiral matrix of the bismuth sublattice, leading to optical activity decrease. Therefore, the TiO_4 tetrahedra will counteract to the BiO_5 polyhedron more strongly and the total optical activity will be lower.

3.3. Holographic characteristics

The diffraction efficiency evolution during holographic recording and readout of Ru doped and undoped BTO crystals at an incident angle $\Theta = 32°$ is shown in Figs. 4 and 5. The recording

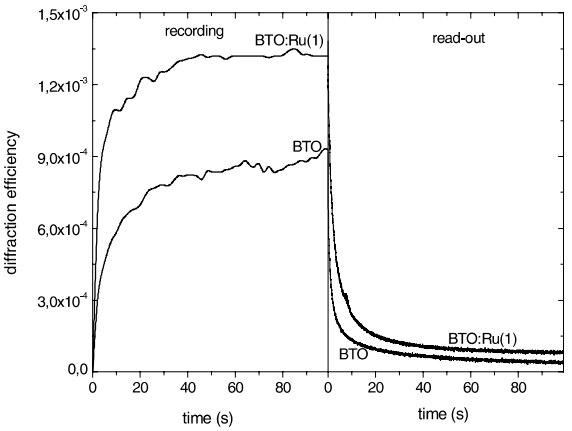

Fig. 4. The diffraction efficiency evolution during holographic recording and readout at incident angle $\Theta = 32°$ of BTO:Ru(1) and undoped BTO crystals.

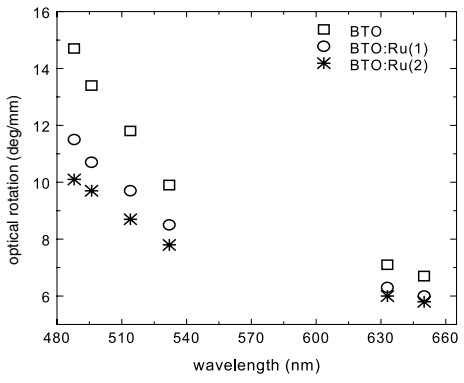

Fig. 3. Optical rotator power dependence on wavelength of doped with different concentration of Ru and undoped BTO crystals.

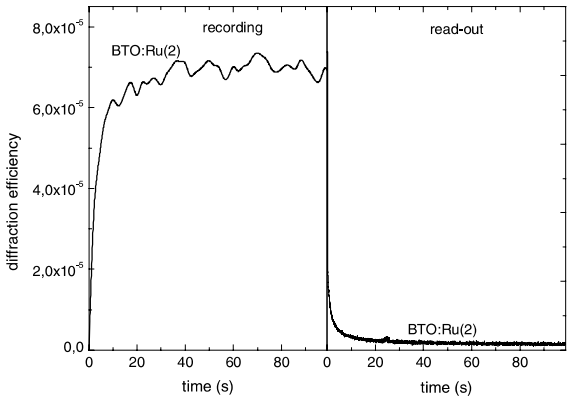

Fig. 5. The diffraction efficiency evolution during holographic recording and readout at incident angle $\Theta = 32°$ of BTO:Ru(2) crystals.

was performed by two coherent beams with the equal intensities of 85 mW/cm^2. As can be seen, in case of ruthenium doped BTO crystals, the diffraction efficiency first increased very fast and after a few seconds reaches a stationary value. A maximum diffraction efficiency is attained in BTO:Ru(1) crystal, being approximately two times as large as that obtained in undoped BTO.

The saturation values of refractive index modulation Δn_s, including absorption, can be deduced using Kogelnik's formula [30]

$$\eta = \exp\left(-\frac{\alpha d}{\cos\theta}\right)\sin^2\left(\frac{\pi\Delta n d}{\lambda\cos\theta}\right), \quad (3)$$

where α is the absorption coefficient, d is the crystal thickness, λ is the vacuum light wavelength, and θ is the angle between the recording beams inside the crystal. The first term (exponential decaying) represents the influence of crystal absorption on the diffraction efficiency and the second term is related to the photorefractive effect and both depend on the impurity concentration. In case of pure refractive index grating with refractive-index amplitude, the first term in Eq. (3) can be neglected. Hence, we have used such approximation to calculate saturation values of refractive index modulation, which for slightly doped BTO crystal is $\Delta n_{sBTO:Ru(1)} = 1 \times 10^{-6}$.

Accordingly in highly doped BTO:Ru(2) crystal due to the observed photochromic effect, probably simultaneously with refractive-index modulation also an absorption grating (modulation of absorption coefficient) is formed. We supposed that such absorption grating originates from the modulation of charge carriers in shallow trap levels. Similar simultaneously presence of two types of gratings was identified and phases and amplitudes of their modulation were determined in Cr-doped BTO [31]. For further estimation of the influence of higher ruthenium doping on BTO photorefractive properties two gratings separation and comparison between absorption and phase contribution to the diffraction efficiency are necessary.

We used a double exponential function of the square root of diffraction efficiency as a function of time: $\sqrt{\eta} = \lfloor\sqrt{\eta_1}(1-\exp(-t/\tau_1)) + \sqrt{\eta_2}(1-\exp(-t/\tau_2))\rfloor$ in order to calculate faster (τ_1) and slower (τ_2) build-up time constants. This function matches the experimental data points quite well. Owing to the higher traps concentration highly Ru doped BTO exhibits faster response time. Experimental data of calculated build-up time constants τ_1 and τ_2 are presented in Table 3.

Table 3
Experimental data of build-up time constants of faster τ_1 and slower τ_2 components

Sample	BTO:Ru(1)	BTO:Ru(2)	BTO
τ_1 (s)	1.2	0.9	2
τ_2 (s)	14	10	22

The recording was performed by two coherent beams with equal intensity of 85 mW/cm^2 and incident angle of $\Theta = 32°$. No external electric field is applied.

Read-out is performed by one of the recording beams. The erasure of the recording gratings also consists of two stages: at the beginning the diffraction efficiency decreases very fast and after that follows an exponential decay law. These two separate decay rates are attributed to the existence of two types of trapping centers involved in the photorefractive charge carrier process [32]. Fig. 6 shows the decay time constants of the second part of the gratings decay as function of spatial frequencies. The dependence on spatial frequencies is an indication for existence of two different kinds of light-induced charge carriers. Obviously, doping with high Ru concentration leads to faster speed during writing and reading. Probably, different

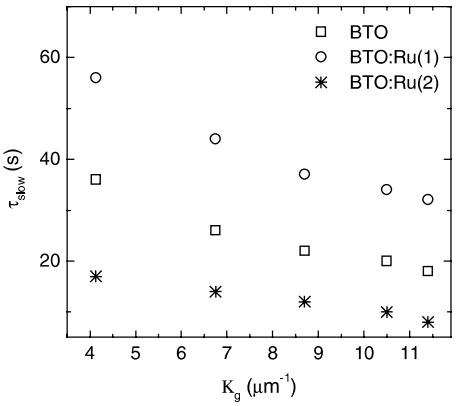

Fig. 6. Decay time constants τ_{slow} of the second part of the gratings decay as function on spatial frequencies K_g. No external electric field is applied.

ruthenium concentrations create different kinds of traps, which are responsible for the refractive index modulation. Additional experiments are necessary to obtain more information about the assumed charge-transport model.

3.4. Role of the ruthenium doping

Several donor and acceptor states are expected to lie in the forbidden band in sillenite crystals. In BTO crystals doped with Ru the band gap structure becomes more complicated, due to the following facts:

- as we mentioned earlier, in BTO exist approximately 10% of Ti^{4+} vacancies in tetrahedral positions, which are replaced by Bi^{3+}-ions, and
- possibilities of ruthenium (4d element) to exist in sillenites [25] in three different valence states Ru^{3+}, Ru^{4+} and Ru^{5+} like Rh (also platinum group metal) in oxide crystals such as $KNbO_3$ and $BaTiO_3$ [12,33].

In general Ru^{4+} can occupy Bi^{3+} in tetrahedral positions, however it also can substitute some Ti^{4+} atoms due to the high distribution coefficient, i.e. the ruthenium concentration in the melt and in the crystal are nearly the same.

Generally Ru^{4+} possess an amphoteric behavior, i.e., it can accept holes or electrons to produce Ru^{5+} or Ru^{3+}, respectively. The absorption band in the bleached color state could be assigned to the transition $Ru^{4+} + e^-_{VB} \rightarrow Ru^{3+}$ (e^-_{VB}-electron from the valence band).

Finally, we suppose that the most probably Ru can replace Bi^{3+}-atoms on Ti^{4+} tetrahedral site vacancies, which are well known to create photorefractive centers in BTO crystals. Perhaps, ruthenium introduced two different levels in BTO forbidden zone-$Ru^{3+/4+}$, which act as shallow trap levels and $Ru^{4+/5+}$ acts as deep trap levels.

4. Conclusion

Our preliminary optical and holographic measurements of ruthenium doped BTO crystals indicate that these properties strongly depend on the Ru concentration. Transmission spectra shift to the longer wavelength, while absorption increases with ruthenium content. Ruthenium doping in BTO also reduces further the optical activity. Photochromic effect was observed in crystals with higher ruthenium concentration. In such crystals, due to the enhanced absorption and photochromic effect, probably an amplitude (absorption) grating is formed during writing together with phase (refractive index) one. In comparison with slightly Ru doped BTO, heavily doped crystals lead to faster response time but to weaker diffraction efficiency. Temporally dynamic erasing curves with faster and slower components indicate that two types of photoactive centers are involved in charge carrier process.

Using an appropriate concentration of ruthenium doping the optical transmission and photorefractive properties of BTO crystals could be changed in the desired direction. The improved properties in the near IR for instance open the direction for investigations towards new possible applications.

Since the photorefractive process in BTO crystals doped with three valence states elements is very complicated, a wide range of different experiments are necessary to obtain an appropriate basis for the physical model.

Acknowledgements

Financial support of the Ministry of Education under grant 89-E-FA06-1-4 and National Science Council under NSC-90-2215-E-009-013, Taiwan R.O.C. are gratefully acknowledged.

References

[1] H. Coufal, G. Sincerbox, D. Psaltis (Eds.), Holographic Data Storage, Springer, New York, 2000.
[2] P. Gunter, J.P. Huignard (Eds.), Photorefractive Materials and Their Applications, vol. I, Springer, Berlin, 1988; Photorefractive Materials and Their Applications, vol. II, Springer, Berlin, 1989.
[3] L. Solymar, D. Webb, A. Grunnet-Jepsen (Eds.), The Physics and Applications of Photorefractive Materials, Clarendon Press, Oxford, 1996.
[4] L. Arizmendi, J. Cabrera, F. Agullo-Lopez, Int. J. Optoelectron. 7 (2) (1992) 149.
[5] A. Feldman, W. Brower, D. Horowitz, Appl. Phys. Lett. 16 (5) (1970) 201.

[6] R.M. Ribeiro, A.B.A. Fiasca, P.A.M. dos Santos, M.R.B. Andreeta, A.C. Hernandes, Opt. Mater. 10 (3) (1998) 201.
[7] S. Riehemann, F. Rickermann, V. Volkov, A. Egorysheva, G. Von Bally, Int. J. Nonlinear Opt. Phys. Mater. 6 (2) (1997) 235.
[8] F. Mersch, K. Buse, W. Sauf, H. Hesse, E. Kratzig, Phys. Stat. Sol. A 140 (1993) 273.
[9] S. Riehemann, D. Dirksen, G. Von Bally, Solid State Commun. 95 (8) (1995) 529.
[10] S. Miyazawa, Opt. Mater. 4 (1995) 192.
[11] V. Marinova, Opt. Mater. 15 (2) (2000) 149.
[12] V. Marinova, M. Veleva, D. Petrova, I. Kourmoulis, D. Papazoglou, A. Apostolidis, E. Vanidhis, N. Deliolanis, J. Appl. Phys. 89 (5) (2001) 2686.
[13] T.S. Yeh, W.J. Lin, I.N. Lin, L.J. Hu, S.P. Lin, S.L. Tu, C.H. Lin, S.E. Hsu, Appl. Phys. Lett. 65 (10) (1994) 1213.
[14] H. Marquet, M. Tapiero, J.C. Merle, J.P. Zielinger, J.C. Jaunay, Opt. Mater. 11 (1998) 53.
[15] J.P. Carvalho, R.W. Franco, C.J. Magon, L.A.D. Nunes, F. Pellegrin, A.C. Hernandes, Mater. Res. 2 (2) (1999) 87.
[16] K. Buse, H. Hesse, U. van Stevendal, S. Loheide, D. Sabbert, E. Kratzig, Appl. Phys. A 59 (1994) 563.
[17] M. Gospodinov, S. Haussuhl, P. Sveshtarov, S. Dobreva, A. Sampil, Mater. Res. Bull. 27 (12) (1992) 1415.
[18] S.C. Abrahams, P.B. Jamieson, I.L. Bernstein, J. Chem. Phys. 47 (1967) 4034.
[19] R. Oberschmid, Phys. Stat. Sol. A 89 (1985) 263.
[20] B.C. Grabmaier, R. Obersmid, Phys. Stat. Sol. A 96 (1986) 199.
[21] V.A. Sarin, E. Rider, V.N. Kanepit, N.N. Bandanov, V.V. Volkov, Y.F. Kargin, V.M. Skorikov, Crystallography 34 (3) (1989) 628.
[22] S. Neov, V. Marinova, M. Reehuis, R. Sonntag, Appl. Phys. A (in press).
[23] H.J. Reyher, U. Hellwig, O. Thiemann, Phys. Rev. B 47 (10) (1993) 5638.
[24] B. Briat, H.J. Reyher, A. Hamri, N.G. Romanov, J.C. Launnay, F. Ramaz, J. Phys. Condens. Matter 7 (34) (1995) 6951.
[25] H. Bou Rjeily, F. Ramaz, D. Petrova, M. Gospodinov, B. Briat, SPIE 3178 (1997) 169.
[26] W. Wardzynski, T. Lukasievicz, J. Zmija, Opt. Commun. 30 (1979) 203.
[27] S. Sainov, M. Gospodinov, S. Sainov, V. Marinova, Opt. Commun. 101 (1993) 5.
[28] V.I. Burkov, Inorg. Mater. 30 (1994) 12.
[29] V.I. Burkov, U.F. Kargin, V.V. Volkov, N.U. Zubovich, Inorg. Mater. 30 (1994) 1078.
[30] H. Kogelnik, Bell Syst. Tech. J. 48 (1969) 2909.
[31] V. Marinova, D. Tonchev, G. Stoilov, N. Metchkarov, V. Sainov, in: ISCMP Xth International School of Condensed Matter Physics, 1999, p. 521.
[32] G.C. Valley, Appl. Opt. 32 (2) (1983) 3160.
[33] H. Krose, R. Scharfschwerdt, O.F. Shirmer, H. Hesse, Appl. Phys. B 61 (1995) 1.